Octanoyl esterification of low molecular weight sulfated galactan enhances the cellular uptake and collagen expression in fibroblast cells

WARAPORN SAKAEW[1], SOMSUDA SOMINTARA[1], KAMONWAN JONGSOMCHAI[2], JAMAL EL-ABID[3], KANOKPAN WONGPRASERT[4], JOSÉ KOVENSKY[5] and TAWUT RUDTANATIP[1]

[1]Electron Microscopy Unit, Department of Anatomy, Faculty of Medicine, Khon Kaen University, Khon Kaen 40002; [2]Division of Anatomy, School of Medical Sciences, University of Phayao, Phayao 56000, Thailand; [3]Department of Organic Chemistry, Arrhenius Laboratory, Stockholm University, Stockholm 10691, Sweden; [4]Department of Anatomy, Faculty of Science, Mahidol University, Bangkok 10400, Thailand; [5]Laboratory of Glycochemistry and Agroresources UR 7378, Picardie Institute of Chemistry FR 3085, University of Picardie Jules Verne, 80000 Amiens, France

Received July 6, 2023; Accepted October 11, 2023

DOI: 10.3892/br.2023.1681

Abstract. Low molecular weight sulfated galactan (LMSG) supplemented with octanoyl ester (Oct-LMSG) demonstrated superior wound healing activity compared to the unsupplemented LMSG in a fibroblast wound model. To test the hypothesis that the increased bioactivity of Oct-LMSG may depend on its penetration into the plasma membrane, its cellular uptake was investigated and collagen production in fibroblast cells was assessed for the first time. The cellular uptake of Oct-LMSG was examined using indirect immunofluorescence and a confocal laser scanning microscope. In addition, the degree of fibroblast activation associated with this uptake was evaluated. The results indicated increased LMSG internalization in fibroblasts treated with Oct-LMSG. Transmission electron micrographs revealed the ultrastructure of active protein production in fibroblasts upon treatment with Oct-LMSG. In addition, Oct-LMSG upregulated the expression of type I collagen mRNA and proteins, as well as related signaling molecules involved in collagen synthesis, including collagen type I α1 chain (Col1A1), Col1A2, phosphorylated (p)-Smad2/3 and p-Smad4. The current findings support the notion that the supplementation of LMSG with octanoyl enhanced its cellular uptake into fibroblasts and, as a result, regulated the expression of type I collagen in fibroblasts via the activation of the Smad signaling pathway. This study demonstrates the therapeutic potential of Oct-LMSG in promoting tissue regeneration.

Correspondence to: Dr Tawut Rudtanatip, Electron Microscopy Unit, Department of Anatomy, Faculty of Medicine, Khon Kaen University, 123 Moo 16 Thanon Mittraphap, Mueang, Khon Kaen 40002, Thailand
E-mail: tawut@kku.ac.th

Key words: low molecular weight sulfated galactan, octanoyl ester, collagen-I, Smad proteins, fibroblasts

Introduction

Wound repair is the result of multiple, well-coordinated events, including hemostasis, inflammation, proliferation and wound remodeling, which are associated with various cellular and humoral mechanistic activities (1). It is well-documented that during the proliferative phase of healing, fibroblast cell proliferation and migration are crucial cellular mechanisms (2). Fibroblasts, which were first described in the context of wound healing, have a role in the synthesis of the extracellular matrix (ECM) and successful granulation tissue formation (3). Collagen is a major protein in the ECM, responsible for supporting cellular structure, stability and elasticity (4). Type I collagen, the most abundant type present in the human body, promotes cell proliferation as well as tissue connection and attachment (5). The synthesis of collagen is regulated by several factors. The transforming growth factor-β (TGF-β) signaling pathway contributes to increased collagen biosynthesis through the phosphorylation within the Smad signaling pathway. Upon phosphorylation of Smad2/3, it complexes with phosphorylated (p)-Smad4. This complex subsequently translocates to the nucleus, activating genes that govern collagen production (6).

Wound treatment remains an important medical and social issue. Numerous individuals worldwide suffer from injuries, burns, ulcers and surgical wounds, the treatment of which requires significant financial and healthcare resources. The search for effective, affordable, easily applicable wound-healing drugs continues to be a pressing issue in modern medicine.

Sulfated polysaccharides (SP) are highly regarded as wound-healing compounds due to their low toxicity, excellent degradability, biocompatibility and wide-ranging pharmaceutical properties (7). For instance, *Eucheuma Cottonii* SP, known for its antioxidant and antibacterial activities, has

proven beneficial in the wound-healing process by preventing further tissue damage and enhancing cell proliferation (8). *Gracilaria lemaneiformis* SP demonstrated accelerated wound healing *in vitro* human keratinocyte HaCaT cells due to improved cell polarity and directed cell migration towards the wound site (9). Furthermore, *Sanguisorba officinalis L*. SP (SOSP) has been utilized for burn wound treatment in mice. These outcomes suggest that SOSP enhances wound healing, potentially through the promotion of collagen synthesis (10). Sulfated galactan (SG) cold-water extracts from *Gracilaria fisheri*, an SP with a complex structure of galactose monosaccharide residues coupled with sulfate ester, exhibit various pharmaceutical properties, including immune regulation (11), antioxidant activity (12), antibacterial characteristics (13) and promotion of wound-healing (14). However, the cellular uptake of many bioactive compounds, such as drugs, may be limited by several factors, including their hydrophobicity and size. Octanoyl esterification can address these limitations by increasing the lipophilicity (fat-solubility) of the compound, enabling improved penetration through the cell membrane (15). A previous study demonstrated that galactose synthesized with octanoyl ester improved its accumulation within the cell and its bioactivity (16). In addition, recent research by our group indicated that a low molecular weight (mw) SG (LMSG) with added octanoyl moiety (Oct-LMSG) exhibited enhanced wound healing activity by activating cell proliferation and migration in both *in vitro* scratched fibroblast studies and *in vivo* excision wound rat models. The improved wound healing observed in the scratched fibroblasts with Oct-LMSG was attributed to the activation of proliferation and migration-related mRNA and proteins (17). In the present study, the hypothesis was tested that octanoyl esterification enhances the membrane-penetrating efficacy of LMSG in fibroblast cells and promotes collagen synthesis, which is an essential molecule in tissue regeneration.

Materials and methods

Oct-LMSG. An octanoyl moiety was added to LMSG (mw, 7.87 kDa) to obtain Oct-LMSG following a previously described protocol (17). The structure of Oct-LMSG, analyzed by Fourier transform infrared and NMR spectroscopy (Fig. S1), consists of the alternative 3-linked β-D-galactopyranose and 4-linked 3,6-anhydro-α-L-galactopyranose or α-L-galactopyranose-6-sulfate containing an octanoyl ester moiety (Fig. 1).

Fibroblast culture and cell viability. L929 fibroblasts purchased from the American Type Culture Collection were cultured in Gibco Minimum Essential Medium (Gibco; Thermo Fisher Scientific, Inc.) containing 2.2 g/l sodium bicarbonate, 10% fetal bovine serum and 1% antibiotic-antimycotic (Gibco; Thermo Fisher Scientific, Inc.) in a humidified incubator containing 5% CO_2 at 37˚C. To determine cell viability, cells were seeded in a 96-well plate ($3x10^4$ cells/well) and incubated with various concentrations of Oct-LMSG (10-1,000 μg/ml) for 24 and 48 h at 37˚C. Subsequently, cell viability was measured with an MTT assay. In brief, the wells containing cells were incubated with 10 μl of medium containing 5 mg/ml MTT (final concentration in the well, 0.5 mg/ml) for 4 h at 37˚C in the dark. The medium was removed and 100 μl dimethyl sulfoxide was added to each well to solubilize formazan crystals in the cells. The absorbance at 595 nm was measured using a Varioskan LUK multimode microplate reader (Thermo Fisher Scientific, Inc.). The viability of cells was expressed as a percentage of the control.

Cellular uptake study. Fibroblasts ($3x10^5$ cells/well) were cultured overnight on poly-L-lysine-coated round-glass coverslips in a 24-well plate and treated with LMSG and Oct-LMSG at a concentration of 100 μg/ml for 12 h at 37˚C. Cells with no treatment served as the control. The coverslips were washed three times (3x10 min) with 100 μl PBS, fixed with 100 μl 4% paraformaldehyde in PBS for 20 min and blocked with 100 μl 1% BSA in PBS for 30 min at room temperature (RT). After washing, the coverslips were incubated with anti-LM5 primary antibody (monoclonal-rat IgG, specific to β-D-galactan; dilution, 1:250; cat. no. LM5-050; Plant Probes) overnight at 4˚C, followed by incubation with the secondary antibody, FITC-conjugated goat anti-rat IgG (dilution, 1:500; cat. no. 31629; Thermo Fisher Scientific, Inc.), for 1 h at RT. The cell nuclei were specifically stained with DAPI. The cytoplasmic and plasma membranes of the cells were stained with CellMask™ Deep Red Plasma Membrane Stain (Thermo Fisher Scientific, Inc.) according to the manufacturer's protocols. Cellular uptake of LMSG and Oct-LMSG was observed under a confocal laser-scanning microscope (Zeiss LSM800; Carl Zeiss AG). In addition, the fluorescent label concentration was assessed by measuring the FITC intensity using a Varioskan LUK multimode microplate reader (Thermo Fisher Scientific, Inc.) to further investigate the cellular uptake of Oct-LMSG in fibroblasts.

Cell-ultrastructure evaluation. After 12 h of treatment, fibroblasts were immediately fixed in Karnovsky's fixative for 30 min at RT. Cells were washed with PBS, centrifuged at 1,500 x g for 1 min at 25˚C and then post-fixed with 1% OsO_4 in 0.1 M phosphate buffer for 1 h at RT. Fixed cells were washed again and centrifuged at 1,500 x g for 1 min at 25˚C. The collected cell pellets were placed in a small cavity in solidified 2% agarose and filled with 2% liquefied agarose. After solidification, the agarose containing the embedded cells was cut into small cubes and dehydrated through a series of ethyl alcohol gradients (at 50, 70, 80, 90 and 95% for 5 min each and 100% for 10 min). The agarose cubes were gently infiltrated with propylene oxide, followed by a mixture of propylene oxide and Epon 812 (1:1), and a mixture of propylene oxide and Epon 812 (1:3) for 10 min each. They were finally infiltrated with pure Epon 812 at RT overnight. The agarose cubes were then embedded in fresh Epon 812 and polymerized at 60˚C for 48 h. Ultra-thin sections were obtained using an Ultracut N ultramicrotome (Reichert-Nissei; Leica Microsystems, Inc.). Sections were stained with 5% uranyl acetate and 2% lead citrate prior to observation under a JEM1010 transmission electron microscope (TEM; JEM-1010; Jeol, Co., Ltd.).

Immunofluorescence. TEM results indicated an increase in vesicles or granules within the cytoplasm of fibroblasts. Therefore, immunofluorescent staining for type I collagen was performed. Cells cultured on coated round-glass coverslips

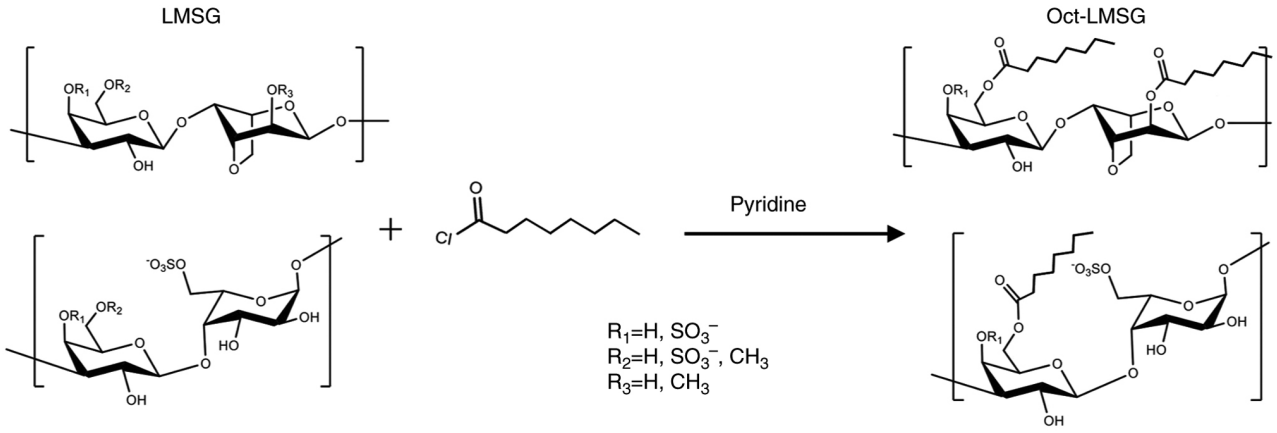

Figure 1. Scheme for reaction of LMSG added with octanoyl moiety and the structural features of Oct-LMSG after reaction. Oct-LMSG, low molecular weight sulfated galactan added with octanoyl moiety.

were divided into three groups: i) Normal control-cells without treatment; ii) Oct-LMSG-cells treated with 100 μg/ml of Oct-LMSG; and iii) TGF-β-cells treated with 10 ng/ml of TGF-β (Sigma-Aldrich; Merck KGaA), a known pro-fibrogenic growth factor that binds with the cell membrane receptors of fibroblasts and mediates type I collagen biosynthesis (6). After 12 h of treatment, cells were incubated with anti-collagen type I α1 chain (Col1A1) antibody (dilution, 1:250; cat. no. A22089; ABclonal Science, Inc.) overnight at 4˚C, followed by incubation with the secondary antibody, FITC-conjugated goat anti-rabbit IgG (dilution, 1:500; cat. no. 701078; Thermo Fisher Scientific, Inc.), for 1 h at RT. As a negative control for immunofluorescent staining, the sample was prepared by omitting the secondary antibody. The cells were counter-stained with DAPI (nuclei) and CellMask™ Deep Red Plasma Membrane (cytoskeleton) according to the manufacturer's protocols. Immunofluorescent images were observed under a fluorescence microscope (Leica DFC 7000T; Leica Microsystems, Inc.).

Expression of type I collagen in fibroblasts. Fibroblasts ($3x10^6$ cells/well) were cultured in a 6-well plate for 24 h and then divided into three groups: i) Normal control-cells without treatment; ii) Oct-LMSG-cells treated with 100 μg/ml Oct-LMSG; and iii) TGF-β-cells treated with 10 ng/ml TGF-β as a positive control. Cells were treated with an Oct-SG or TGF-β solution (2 ml) and further incubated for 6, 12 and 24 h before being harvested for RNA and protein extractions.

RNA was extracted from cultured cells using 200 μl of TRI Reagent® RNA Isolation Reagent (Sigma-Aldrich; Merck KGaA) according to the manufacturer's protocol. The concentration and quality of RNA was measured by determining the absorbance ratio at 260/280 nm using a NanoDrop 2000 spectrophotometer (Thermo Fisher Scientific, Inc.). RNA (1 μg) was converted to cDNA using the Revert Aid First Strand cDNA Synthesis Kit (Thermo Fisher Scientific, Inc.). Subsequently, mRNA transcription of Col1A1, Col1A2 and GAPDH was amplified by quantitative (q)PCR using 2 μl of cDNA with specific primers and conditions. The qPCR conditions included initial denaturation at 95˚C for 10 min, followed by 40 cycles at 95˚C for 10 sec, 60˚C for 30 sec and 72˚C for 30 sec. Col1A1-specific primers were 5'-GAGAGGTGAACA AGGTCGCG-3' (forward) and 3'-AAACCTCTCTCGCCT CTTGC-5' (reverse), Col1A2-specific primers were 5' CCC AGAGTGGAACAGCGATT-3' (forward) and 3'-ATGAGT TCTTCGCTGGGGTG-5' (reverse), and GAPDH-specific primers were 5'-GGTGAAGGTCGGTGTGAA-3' (forward) and 3'-CTCGCTCCTGGAAGATGGTG-5' (reverse) (14). The amplification and analysis were performed on a QuantStudio™ 6 Flex Real-Time PCR System device (Applied Biosystems; Thermo Fisher Scientific, Inc.). The relative gene expression in the different samples was calculated using the $2^{-\Delta\Delta Cq}$ method (18). The relative mRNA transcription levels were normalized to the GAPDH internal control and presented as a fold-change relative to the control.

Proteins were extracted from the cells using a lysis buffer containing 100X protease inhibitor solution (MedChemExpress, LLC). The protein concentration was determined using a NanoDrop 2000 spectrophotometer (Thermo Fisher Scientific, Inc.). Proteins (40 μg/lane) were then separated by 12%-SDS-PAGE and transferred to a nitrocellulose membrane (Sigma-Aldrich; Merck KGaA). The membrane was incubated with specific primary antibodies for Col1A1 (cat. no. A22089; ABclonal Science, Inc.), Col1A2 (cat. no. A21059; ABclonal Science, Inc.), Smad2/3 (cat. no. 8685; Cell Signaling Technology, Inc.), Smad4 (cat. no. 46535; Cell Signaling Technology, Inc.), p-Smad2/3 (cat. no. 8828; Cell Signaling Technology, Inc.) and p-Smad4 (cat. no. AF8316; Affinity Biosciences, Inc.) at a dilution of 1:1,000 at 4˚C overnight, followed by incubation with HRP-conjugated secondary antibodies, anti-mouse IgG (cat. no. 62-6520; AB_2533947) and anti-rabbit IgG (cat. no. 31460; AB_228341; Thermo Fisher Scientific, Inc.) at a dilution of 1:2,000 for 1 h at RT. Immunoreactive protein bands were visualized using the Clarity™ Western ECL substrate (Bio-Rad Laboratories, Inc.). The relative protein expression was normalized to β-actin as the internal control (cat. no. AF7018; Affinity Biosciences, Inc.) and presented as a fold-change relative to the control. Protein expression was quantified by ImageJ 1.46r analysis software (National Institutes of Health).

Statistical analysis. Data are presented as the mean ± standard error of the mean from three or more independent experiments.

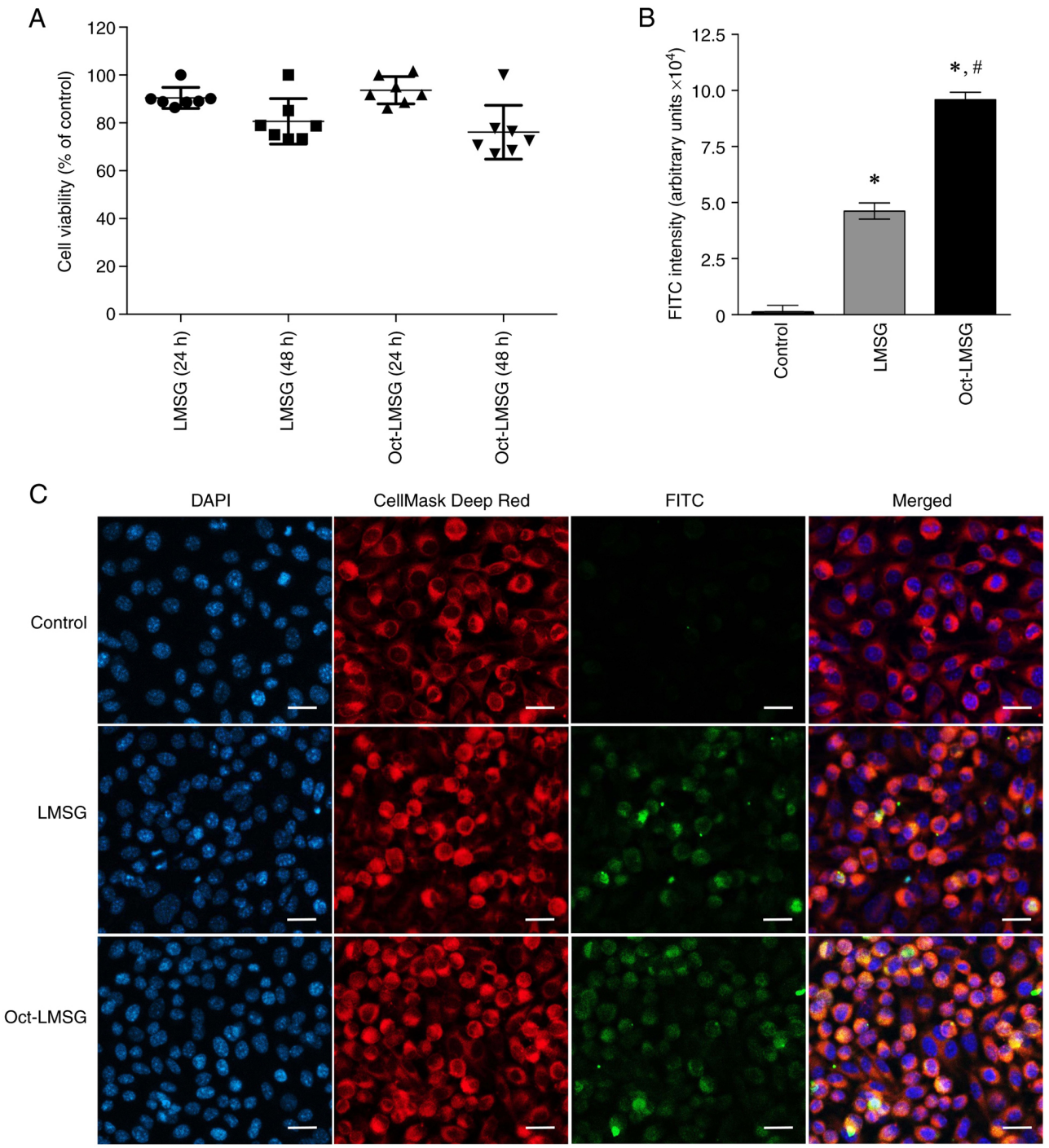

Figure 2. Cytotoxicity and cellular uptake study of Oct-LMSG in L929 fibroblasts. (A) Cytotoxicity effect of LMSG and Oct-LMSG on L929 fibroblasts cultured for 24 and 48 h, as measured by MTT assay and (B) the graphs represent the fluorescent intensity value of FITC-conjugated LMSG in fibroblasts detected by spectrofluorometer. Data are presented as the mean ± standard error or the mean of three independent experiments. *P<0.05 vs. control; and #P<0.05 vs. LMSG. (C) Confocal laser scanning micrographs showing the presence of FITC-conjugated LMSG in L929 fibroblasts after treatment with LMSG and Oct-LMSG at the concentration of 100 μg/ml for 12 h (scale bar, 20 μm). Oct-LMSG, low molecular weight sulfated galactan added with octanoyl moiety.

All treated groups were compared with the control groups. Statistical significance was analyzed using one-way ANOVA followed by Tukey's multiple-comparisons test. P<0.05 was considered to indicate a statistically significant difference.

Results

Increased cellular uptake of Oct-LMSG. The cytotoxicity of LMSG and Oct-LMSG to fibroblasts, as determined by the MTT assay, indicated that there was no significant cytotoxicity, and no difference between groups was observed after 24 and 48 h of incubation (Fig. 2A). To validate the hypothesis that addition of the octanoyl moiety could mediate increases in LMSG uptake into fibroblasts, an indirect immunofluorescent labelling technique was performed and the FITC intensity was quantified. As presented in Fig. 2C, the cells treated with LMSG and Oct-LMSG followed by FITC labelling displayed green fluorescence bound to the cells and localized within the

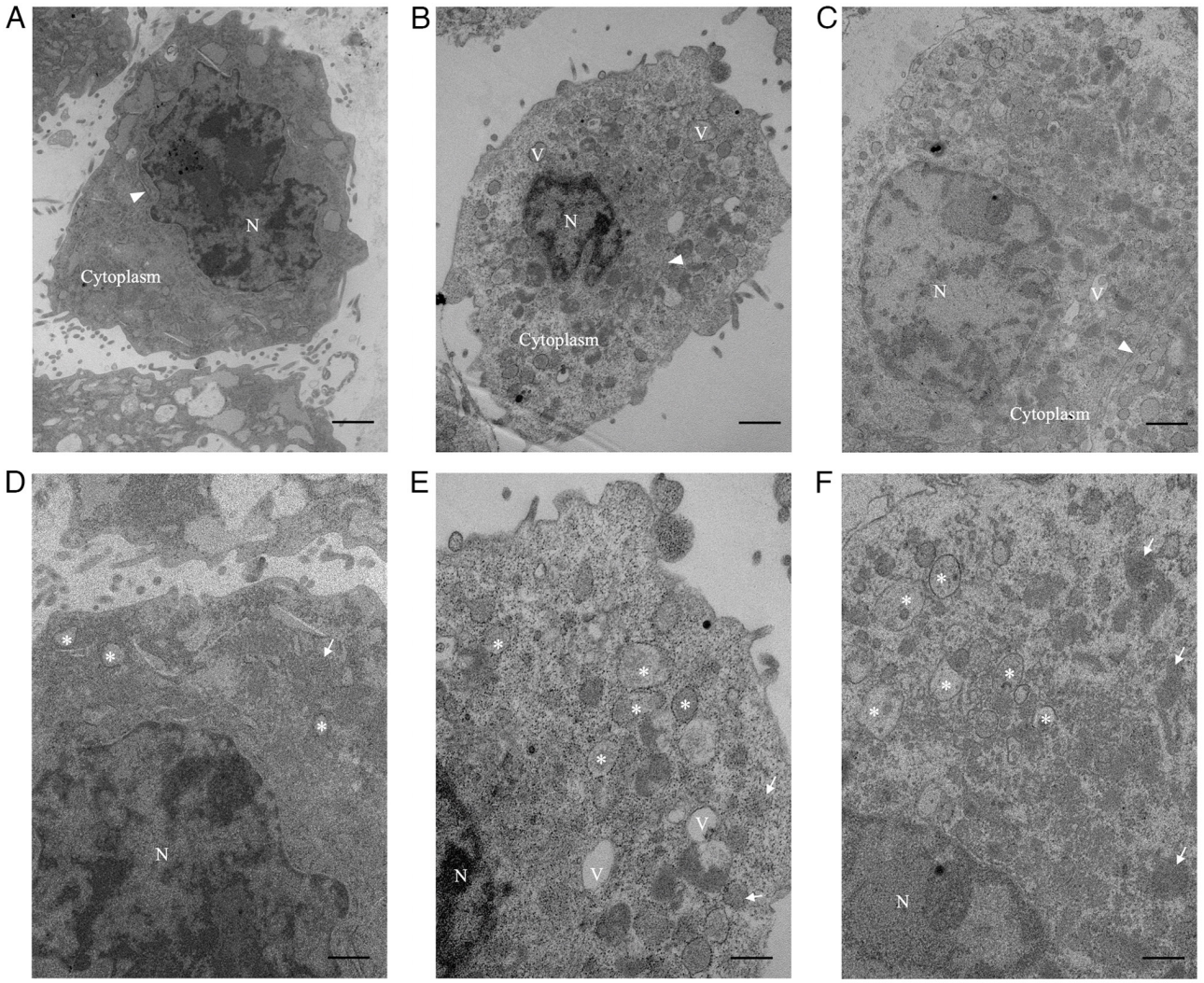

Figure 3. TEM images showing the cultured L929 fibroblasts after Oct-LMSG and TGF-β treatment. Low-magnification TEM of (A) control fibroblasts, (B) Oct-LMSG-treated fibroblasts and (C) TGF-β-treated fibroblasts. High-magnification TEM of (D) control fibroblasts, (E) Oct-LMSG treated fibroblasts and (F) TGF-β treated fibroblasts (scale bars: Low magnification, 1 μm; high magnification, 500 nm). N, nucleus; V, vacuole; arrowhead, rough endoplasmic reticulum; arrow, mitochondria; asterisk, vesicle; Oct-LMSG, low molecular weight sulfated galactan added with octanoyl moiety; TEM, transmission electron microscopy.

cytoplasm (orange color dispersed in the cytoplasm shown in merged micrographs). No green fluorescence was detected in the control cells. The FITC-LMSG fluorescence intensity of LMSG- and Oct-LMSG-treated cells was $4.69\pm0.89\text{x}10^4$ and $9.71\pm0.64\text{x}10^4$ arbitrary units, respectively (Fig. 2B). Comparison between LMSG and Oct-LMSG revealed that the introduction of the octanoyl moiety increased the uptake of LMSG into fibroblasts, suggesting that the cellular uptake of LMSG was enhanced by octanoyl supplementation.

Ultrastructural changes of fibroblasts by Oct-LMSG treatment. TEM analysis was performed to assess the ability of Oct-LMSG to affect the ultrastructure of L929 fibroblasts. It was noted that cultured fibroblasts in the control group exhibited a small oval body occupied by the nucleus of a heterochromatin structure and encircled by a small amount of cytoplasm (Fig. 3A). In addition, high-magnification images of these controls showed that the cytoplasm was filled with sparse vesicles containing pale particles, rough endoplasmic reticulum (rER) and mitochondria (Fig. 3D). By contrast, fibroblasts cultured with Oct-LMSG and TGF-β displayed primarily euchromatin nuclear features and were surrounded by an extensive cytoplasmic medium containing abundant vesicles, vacuoles and free ribosomes (Fig. 3B and C). Under high magnification, these vesicles, which appeared to be dilated cisternae of the rER, exhibited morphological differences from those of the control group, containing dense and dark materials (Fig. 3E and F). The presence of euchromatic nuclear features, increased rER-dilated cisternae and free ribosomes in the cytoplasm of fibroblasts treated with Oct-LMSG indicated that Oct-LMSG could activate fibroblasts in a similar manner to TGF-β.

Oct-LMSG enhances the synthesis of type I collagen. To investigate the effect of Oct-LMSG on the synthesis of type I collagen in L929 fibroblasts, cells were initially exposed to Oct-LMSG (100 μg/ml) for 6, 12 and 24 h. Cells were also treated with TGF-β (10 ng/ml), a growth factor that induces the synthesis of collagen in fibroblasts (19). Col1A1 and Col1A2 mRNA transcription following treatment were measured

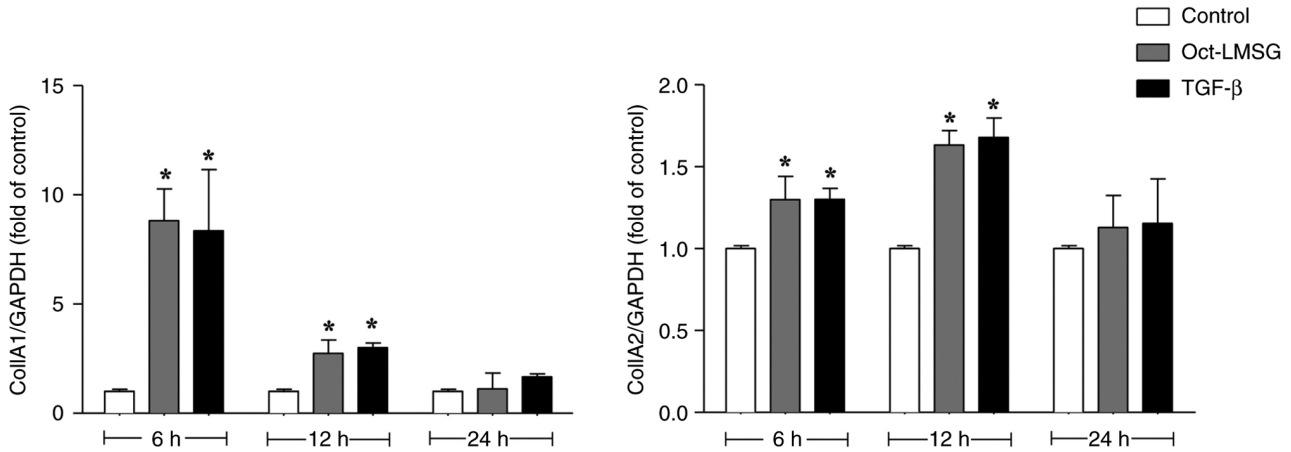

Figure 4. Effect of Oct-LMSG on type I collagen mRNA transcription in L929 fibroblasts. The mRNA levels of Col1A1 and Col1A2 were determined by reverse transcription-quantitative PCR assay after treatment with either Oct-LMSG (100 μg/ml) or TGF-β (10 ng/ml) for 6, 12 and 24 h relative to GAPDH. Values are expressed as the mean ± standard error of the mean of three independent experiments. *P<0.05 vs. control. Oct-LMSG, low molecular weight sulfated galactan added with octanoyl moiety; Col1A1, collagen type I α1 chain.

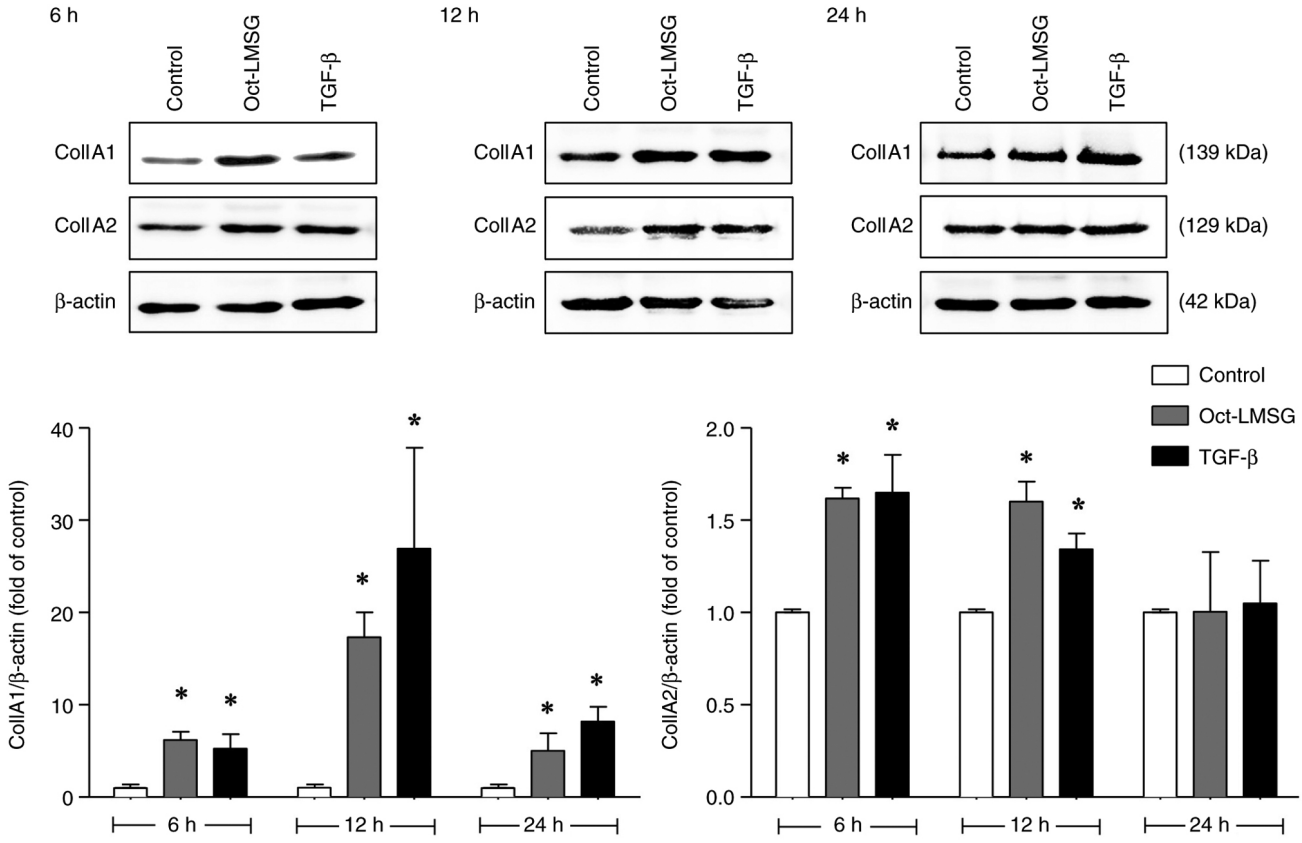

Figure 5. Effect of Oct-LMSG on type I collagen protein expression in L929 fibroblasts. The Col1A1 and Col1A2 protein levels were detected by western blot assay after treatment with either Oct-LMSG (100 μg/ml) or TGF-β (10 ng/ml) for 6, 12 and 24 h relative to β-actin. Values are expressed as the mean ± standard error of the mean of three independent experiments. *P<0.05 vs. control. Oct-LMSG, low molecular weight sulfated galactan added with octanoyl moiety; Col1A1, collagen type I α1 chain.

via reverse transcription-qPCR analysis. As presented in Fig. 4, Oct-LMSG and TGF-β significantly elevated mRNA transcription levels of Col1A1 and Col1A2. The stimulatory effect of Oct-LMSG on collagen mRNA transcription was more pronounced at 6-12 h of incubation and tapered off to control levels at the 24-h mark. Following this, the effect of the Oct-LMSG on protein expression was determined by western blot analysis. As with mRNA transcription levels, exposure to Oct-LMSG increased expression of type I collagen proteins (Col1A1 and Col1A2; Fig. 5), particularly Col1A1 protein expression, which demonstrated a higher expression level that was sustained throughout the first 24 h of incubation compared to the control. In addition, Col1A1-immunofluorescent staining was performed to confirm collagen synthesis in the

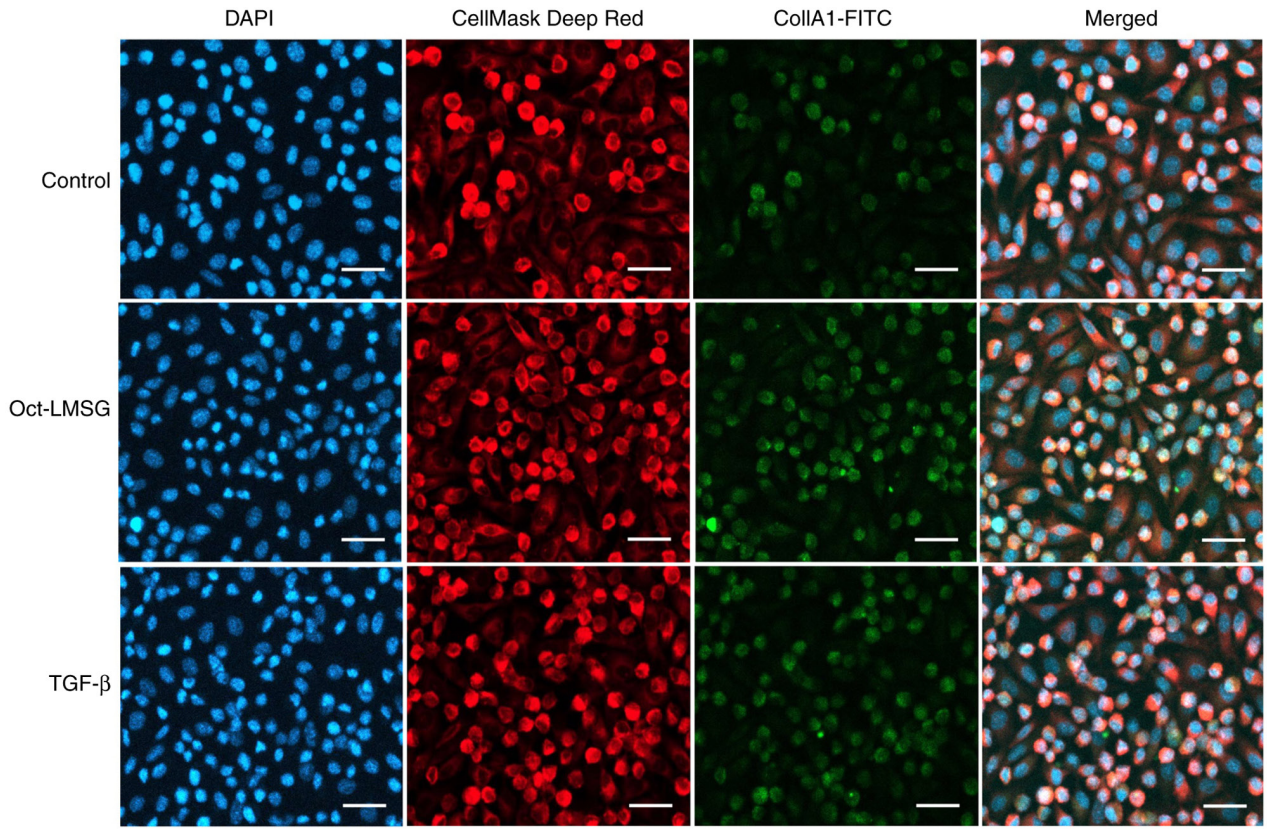

Figure 6. Effect of Oct-LMSG on collagen production in L929 fibroblasts. The collagen synthesis was observed by Col1A1-immunofluorescence staining assay. Fluorescent micrographs of Col1A1-stained fibroblasts. Cells were treated with either Oct-LMSG (100 μg/ml) or TGF-β (10 ng/ml) for 12 h and stained with Col1A1, followed by secondary conjugation with FITC antibodies. Cells were counterstained with DAPI (nucleus) and CellMask Deep Red (cell cytoskeleton). Collagen-Col1A1 is represented by fluorescent green, DAPI by fluorescent blue and CellMask Deep Red by fluorescent red. The negative control was prepared by omission of the secondary antibody, resulting in the absence of fluorescent green (data not shown). Merged fluorescent micrographs are also provided (scale bars, 75 μm). Oct-LMSG, low molecular weight sulfated galactan added with octanoyl moiety; Col1A1, collagen type I α1 chain.

fibroblasts. The result showed heightened fluorescein activity in Oct-LMSG and TGF-β-treated fibroblasts compared to the control (Fig. 6), indicating that increased collagen synthesis was induced by Oct-LMSG. Taken together, these results suggest that Oct-LMSG enhances the expression of type I collagen *in vitro*.

Oct-LMSG activates the phosphorylation of Smad2/3/4 proteins in fibroblasts. Given that the TGF-β/Smad signaling pathway is crucial in regulating Col1A1 synthesis (6), the phosphorylation status of Smad proteins after Oct-LMSG treatment was analyzed. The results indicated that p-Smad2/3 and p-Smad4 were upregulated after Oct-LMSG treatment relative to controls and that the upregulated phosphorylation had no effect on total protein levels, except for Smad2/3 at 12 h of incubation (Fig. 7). These findings were consistent with those of fibroblasts treated with TGF-β. Oct-LMSG significantly upregulated p-Smad2/3 levels to 3.5±0.7-fold of the control at 6 h, 9.3±1.2-fold of control at 12 h and 2.9±0.3-fold of the control at 24 h of incubation. Concurrently, p-Smad4 levels also increased significantly with Oct-LMSG treatment to 1.9±0.1-fold of the control at 6 h, 4.9±0.9-fold of the control at 12 h and 1.8±0.2-fold of the control at 24 h of incubation. These results indicated that Oct-LMSG enhances type I collagen synthesis, at least in part, mediated by the phosphorylation of the Smad signaling pathway in fibroblasts.

Discussion

Wound healing is a complex process that involves the interaction of cells, the extracellular matrix (ECM) and numerous growth factors. Collagen fibers have an important role in wound repair by recruiting fibroblasts and promoting the deposition of new collagen in the injured tissues (20). Increased collagen expression is known to significantly enhance tissue recovery and appearance (21). Several studies have shown that SPs derived from algae, such as *Hizikia fusiforme* (22), *Fucus vesiculosus* (23) and *Gracilaria fisheri* (14), promote type I collagen synthesis and facilitate tissue healing. Furthermore, it has been observed that galactose conjugated with octanoyl ester markedly enhances cellular uptake and bioactivity (16). A recent study by our group reported that Oct-LMSG was able to enhance wound healing activity both *in vitro* and *in vivo* by stimulating the proliferation and migration of fibroblasts (17). However, it has remained elusive whether Oct-LMSG can penetrate the plasma membrane and has a potential role in promoting type I collagen synthesis in fibroblasts. Therefore, the aim of the present study was to investigate the ability of Oct-LMSG to permeate the plasma membrane and regulate the expression of type I collagen mRNA and protein in L929 fibroblast cultures. The underlying signaling pathway of Oct-LMSG in promoting collagen synthesis was also unraveled.

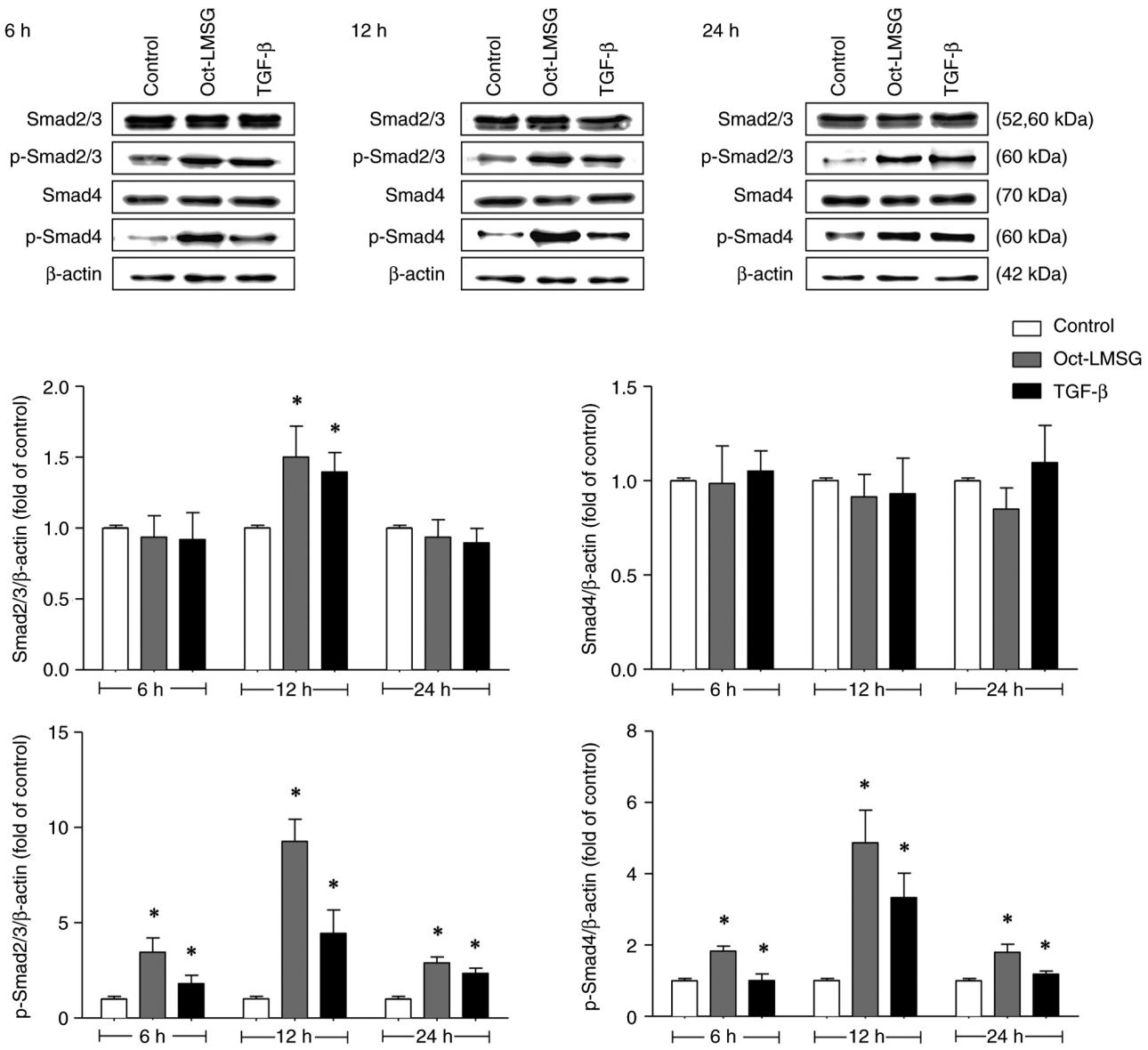

Figure 7. Effect of Oct-LMSG on Smad signaling protein expression in L929 fibroblasts. Smad2/3, Smad4, p-Smad2/3 and p-Smad4 protein levels were detected by western blot assay after treatment with either Oct-LMSG (100 μg/ml) or TGF-β (10 ng/ml) for 6, 12 and 24 h relative to β-actin. The values are expressed as the mean ± standard error of the mean of three independent experiments. *P<0.05 vs. control. Oct-LMSG, low molecular weight sulfated galactan added with octanoyl moiety; p-Smad4, phosphorylated Smad4.

Conjugation of polysaccharides with delivery agents has been shown to enhance their pharmacological properties by increasing cellular uptake. For instance, in Hela cells, enhanced cellular uptake was observed when SPs from *Codium fragile* were conjugated with a selective drug delivery agent, folic acid (24). Similarly, the cellular uptake of hyaluronic acid (HA) was significantly increased in lung cancer cells when HA oligosaccharides were conjugated to a polyethylene glycol-phospholipid (25). The impact of medium-chain fatty acid conjugated polysaccharides on cellular uptake has also been demonstrated. Modification of the coix seed component microemulsion (C-ME) with Oct-galactose ester significantly increased C-ME uptake in HepG2 cells, suggesting that the galactose ester with medium chain fatty acids provided a significant advantage in cellular uptake (16). This finding aligns with the present study, which demonstrated that Oct-LMSG increases cellular uptake into L929 fibroblasts. Furthermore, Oct-LMSG exhibited green fluorescence on the cell surface, suggesting that LMSG probably interacted or bound to protein receptors on the cell membrane (26). However, the interaction between LMSG and protein receptors on the fibroblast cell membrane warrants further investigation.

In the present study, TEM was performed to investigate the impact of Oct-LMSG on the ultrastructure of fibroblasts. The findings demonstrated that fibroblasts cultured with Oct-LMSG exhibited changes in cytoplasmic organelles. These changes included a prominent euchromatic nucleus, dilated cisternae of the rER and increased presence of free ribosomes. These alterations are typically associated with active fibroblasts. Previous studies have documented that active fibroblasts can be identified under TEM by their abundant rER, free ribosomes and prominent Golgi apparatus, all indicative of cells involved in protein synthesis (27). They also exhibited large and irregular nuclei with abundant euchromatin (28). These characteristics align with earlier

research (29) indicating that the calcium hydroxylapatite filler affected the cytoplasmic organelles of fibroblasts, particularly the rER profiles, which consist of ribosome-bound membranes that often form dilated cisternae filled with electron-dense, finely filamentous material. These alterations in the cytoplasm suggest fibroblast activation, leading to the production of molecular precursors of fibrillar components, primarily collagen, for the ECM (29). The specific changes in the ultrastructural features in the present study support the hypothesis that Oct-LMSG activates fibroblasts. Furthermore, TEM images of cultured fibroblasts treated with Oct-LMSG revealed the presence of cytoplasmic vacuoles, suggesting that the compound may be internalized through either endocytosis or macropinocytosis (19).

Collagen, a major protein in the ECM produced by fibroblasts, has a crucial role in providing structural support, strength and elasticity to tissues (4). Among the different types of collagens, type I collagen is the most abundant in the human body and is composed of the Col1A1 and Col1A2 proteins (30). A previous study indicated that Col1A1 is predominantly expressed in fibroblasts, with a higher production ratio compared to Col1A2 (ratio, 2:1) (31). In the present study, the stimulatory effect of Oct-LMSG on the mRNA and protein levels of both Col1A1 and Col1A2 was confirmed, particularly on the significant increase in Col1A1 at 12 h compared to the control. This finding indicates that Oct-LMSG sustains the stimulation of type I collagen expression. In a previous study by our group, it was demonstrated that increased collagen production by SG was a result of elevated Col1A1 mRNA expression (14). The findings from our group are consistent with other studies, which have shown enhanced Col1A1 mRNA levels and collagen type I protein synthesis in Hs27 human dermal fibroblasts treated with emodin for 12 h (32). In addition, treatment of SPs from *Hizikia fusiforme* improved collagen synthesis and protected against UVB-induced collagen degradation (22). However, these findings suggest that collagen biosynthesis may vary depending on the cell type and culture conditions.

The TGF-β/Smad signaling pathway has a role in increasing collagen production by inducing the phosphorylation of Smad2 and Smad3. When Smad2/3 is phosphorylated, it forms a complex with p-Smad4, which then moves into the nucleus to activate target genes responsible for producing procollagen, such as Col1A1 and Col1A2 (6). In the present study, the effects of Oct-LMSG on type I collagen through the TGF-β/Smad signaling pathway were compared with those of exogenous TGF-β protein and it was found that Oct-LMSG can penetrate fibroblast cells and activate the TGF-β/Smad signaling pathway by phosphorylation. Several studies have indicated that various compounds enhance type I collagen expression through the TGF-β/Smad signaling pathway, such as *Pyropia yezoensis*, a marine seaweed (33), and poly-L-lactic acid (34). Furthermore, the present data indicate that Oct-LMSG specifically activates Smad2/3 and Smad4 by causing their phosphorylation, leading to increased expression of Col1A1 and Col1A2. As a result, Oct-LMSG shows potential as a candidate for promoting type I collagen synthesis in the pharmaceutical and cosmetic industries.

In conclusion, in the present study, it was demonstrated that Oct-LMSG had significantly enhanced cellular uptake efficacy as compared with LMSG in L929 fibroblasts. Furthermore, Oct-LMSG was found to increase the expression of type I collagen mRNA and protein by activating the phosphorylation of the Smad signaling pathway. These findings suggest that Oct-LMSG can be used to stimulate collagen synthesis. However, wound healing is a complex process related to numerous systemic cellular and humoral actions. The effects of Oct-LMSG on different cell types require further investigation.

Acknowledgements

The authors would like to acknowledge Dr Dylan Southard from the KKU Publication Clinic (Thailand) for editing the manuscript.

Funding

This work was financially supported by the Office of the Permanent Secretary at the Ministry of Higher Education, Science, Research and Innovation and the Thailand Science Research and Innovation (grant no. RGNS 64-044), the National Research Council of Thailand (NRCT; grant no. N42A650206) and the Khon Kaen University Faculty of Medicine Invitation Research fund (grant no. IN66028).

Availability of data and materials

The datasets used and/or analyzed during the current study are available from the corresponding author on reasonable request.

Authors' contributions

WS, KJ, KW, JK and TR conceived and designed the study. WS, KJ and TR performed the experiments. WS, KJ, JEA, SS, KW, JK and TR were responsible for the analysis of data. WS, KJ, JEA, SS and TR participated in the drafting of the manuscript. KW, JK and TR edited and finalized the draft of the manuscript. KW and JK supervised the study. TR provided funding and project administration. WS, KJ and TR confirm the authenticity of all the raw data. All authors have read and approved the final manuscript.

Ethics approval and consent to participate

Not applicable.

Patient consent for publication

Not applicable.

Competing interests

The authors declare that they have no competing interests.

References

1. Wilkinson HN and Hardman MJ: Wound healing: cellular mechanisms and pathological outcomes. Open Biol 10: 200223, 2020.
2. Addis R, Cruciani S, Santaniello S, Bellu E, Sarais G, Ventura C, Maioli M and Pintore G: Fibroblast proliferation and migration in wound healing by phytochemicals: Evidence for a novel synergic outcome. Int J Med Sci 17: 1030-1042, 2020.

3. Diller RB and Tabor AJ: The role of the extracellular matrix (ECM) in wound healing: A review. Biomimetics 7: 87, 2022.
4. de Araújo R, Lôbo M, Trindade K, Silva DF and Pereira N: Fibroblast growth factors: A controlling mechanism of skin aging. Skin Pharmacol Physiol 32: 275-282, 2019.
5. Irawan V, Sung TC, Higuchi A and Ikoma T: Collagen scaffolds in cartilage tissue engineering and relevant approaches for future development. Tissue Eng Regen Med 15: 673-697, 2018.
6. Xue N, Liu Y, Jin J, Ji M and Chen X: Chlorogenic acid prevents UVA-induced skin photoaging through regulating collagen metabolism and apoptosis in human dermal fibroblasts. Int J Mol Sci 23: 6941, 2022.
7. Kang J, Jia X, Wang N, Xiao M, Song S, Wu S, Li Z, Wang S, Cui SW and Guo Q: Insights into the structure-bioactivity relationships of marine sulfated polysaccharides: A review. Food Hydrocoll 123: 107049, 2022.
8. Teo BSX, Gan RY, Abdul Aziz S, Sirirak T, Mohd Asmani MF and Yusuf E: In vitro evaluation of antioxidant and antibacterial activities of Eucheuma Cottonii extract and its in vivo evaluation of the wound-healing activity in mice. J Cosmet Dermatol 20: 993-1001, 2021.
9. Veeraperumal S, Qiu HM, Zeng SS, Yao WZ, Wang BP, Liu Y and Cheong KL: Polysaccharides from Gracilaria lemaneiformis promote the HaCaT keratinocytes wound healing by polarized and directional cell migration. Carbohydr Polym 241: 116310, 2020.
10. Zhang H, Chen J and Cen Y: Burn wound healing potential of a polysaccharide from Sanguisorba officinalis L. in mice. Int J Biol Macromol 112: 862-867, 2018.
11. Wongprasert K, Rudtanatip T and Praiboon J: Immunostimulatory activity of sulfated galactans isolated from the red seaweed Gracilaria fisheri and development of resistance against white spot syndrome virus (WSSV) in shrimp. Fish Shellfish Immunol 36: 52-60, 2014.
12. Rudtanatip T, Pariwatthanakun C, Somintara S, Sakaew W and Wongprasert K: Structural characterization, antioxidant activity, and protective effect against hydrogen peroxide-induced oxidative stress of chemically degraded Gracilaria fisheri sulfated galactans. Int J Biol Macromol 206: 51-63, 2022.
13. Rudtanatip T, Boonsri N, Asuvapongpatana S, Withyachumnarnkul B and Wongprasert K: A sulfated galactans supplemented diet enhances the expression of immune genes and protects against Vibrio parahaemolyticus infection in shrimp. Fish Shellfish Immunol 65: 186-197, 2017.
14. Pariwatthanakun C, Rudtanatip T, Boonsri B, Pratoomthai B and Wongprasert K: In vitro evaluation of wound healing potential of sulfated galactans from red alga Gracilaria fisheri in fibroblast cells. Songklanakarin J Sci Technol 43: 1374-1381, 2021.
15. Layek B and Singh J: N-hexanoyl, N-octanoyl and N-decanoyl chitosans: Binding affinity, cell uptake, and transfection. Carbohydr Polym 89: 403-410, 2012.
16. Qu D, Liu M, Huang M, Wang L, Chen Y, Liu C and Liu Y: Octanoyl galactose ester-modified microemulsion system self-assembled by coix seed components to enhance tumor targeting and hepatoma therapy. Int J Nanomed 12: 2045-2059, 2017.
17. Rudtanatip T, Somintara S, Sakaew W, El-Abid J, Cano ME, Jongsomchai K, Wongprasert K and Kovensky J: Sulfated galactans from Gracilaria fisheri with supplementation of octanoyl promote wound healing activity in vitro and in vivo. Macromol Biosci 22: e2200172, 2022.
18. Livak KJ and Schmittgen TD: Analysis of relative gene expression data using real-time quantitative PCR and the 2(-Delta Delta C(T)) method. Methods 25: 402-408, 2001.
19. Rakshit M, Gautam A, Toh LZ, Lee YS, Lai HY, Wong TT and Ng KW: Hydroxyapatite particles induced modulation of collagen expression and secretion in primary human dermal fibroblasts. Int J Nanomed 15: 4943-4956, 2020.
20. Chattopadhyay S and Raines RT: Review collagen-based biomaterials for wound healing. Biopolymers 101: 821-833, 2014.
21. Ganceviciene R, Liakou AI, Theodoridis A, Makrantonaki E and Zouboulis CC: Skin-anti-aging strategies. Dermatoendocrinol 4: 308-319, 2012.
22. Wang L, Lee W, Oh JY, Cui YR, Ryu B and Jeon YJ: Protective effect of sulfated polysaccharides from celluclast-assisted extract of Hizikia fusiforme against ultraviolet B-induced skin damage by regulating NF-kB, AP-1, and MAPKs signaling pathways in vitro in human dermal fibroblasts. Mar Drugs 16: 239, 2018.
23. Song YS, Li H, Balcos MC, Yun HY, Baek KJ, Kwon NS, Choi HR, Park KC and Kim DS: Fucoidan promotes the reconstruction of skin equivalents. Korean J Physiol Pharmacol 18: 327-331, 2014.
24. Li CS, Palanisamy S, Talapphet N, Cho M and You SG: Preparation and characterization of folic acid conjugated sulfated polysaccharides on NK cell activation and cellular uptake in Hela cells. Carbohydr Polym 254: 117250, 2021.
25. Cano ME, Lesur D, Bincoletto V, Gazzano E, Stella B, Riganti C, Arpicco S and Kovensky J: Synthesis of defined oligohyaluronates-decorated liposomes and interaction with lung cancer cells. Carbohydr Polym 248: 116798, 2020.
26. Rudtanatip T, Withyachumnarnkul B and Wongprasert K: Sulfated galactans from Gracilaria fisheri bind to shrimp haemocyte membrane proteins and stimulate the expression of immune genes. Fish Shellfish Immunol 47: 231-238, 2015.
27. McAnulty RJ: Fibroblasts and myofibroblasts: Their source, function and role in disease. Int J Biochem Cell Biol 39: 666-671, 2007.
28. Repiskà V, Varga I, Lehocký I, Böhmer D, Blaško M, Polák Š, Adamkov M and Danišovič Ľ: Biological and morphological characterization of human neonatal fibroblast cell culture B-HNF-1. Biologia 65: 919-924, 2010.
29. Zerbinati N, D'Este E, Parodi PC and Calligaro A: Microscopic and ultrastructural evidences in human skin following calcium hydroxylapatite filler treatment. Arch Dermato Res 309: 389-396, 2017.
30. Martinez-Lozano E, Beeram I, Yeritsyan D, Grinstaff MW, Snyder BD, Nazarian A and Rodriguez EK: Management of arthrofibrosis in neuromuscular disorders: A review. BMC Musculoskelet Disord 23: 725, 2022.
31. Sawamura S, Makino K, Ide M, Shimada S, Kajihara I, Makino T, Jinnin M and Fukushima S: Elevated alpha 1(I) to alpha 2(I) collagen ratio in dermal fibroblasts possibly contributes to fibrosis in systemic sclerosis. Int J Mol Sci 23: 6811, 2022.
32. Song P, Jo HS, Shim WS, Kwon YW, Bae S, Kwon Y, Azamov B, Hur J, Lee D, Ryu SH and Yoon JH: Emodin induces collagen type I synthesis in Hs27 human dermal fibroblasts. Exp Ther Med 21: 420, 2021.
33. Kim CR, Kim YM, Lee MK, Kim IH, Choi YH and Nam TJ: Pyropia yezoensis peptide promotes collagen synthesis by activating the TGF-β/Smad signaling pathway in the human dermal fibroblast cell line Hs27. Int J Mol Med 39: 31-38, 2017.
34. Zhu W and Dong C: Poly-L-Lactic acid increases collagen gene expression and synthesis in cultured dermal fibroblast (Hs68) through the TGF-β/Smad pathway. J Cosmet Dermatol 22: 1213-1219, 2023.